Zhang, Q., Zhang, D., Dobah, Y., Scarpa, F., Fraternali, F., & Skelton, R. (2018). Tensegrity cell mechanical metamaterial with metal rubber. *Applied Physics Letters*, *113*(3), [031906]. https://doi.org/10.1063/1.5040850

Tensegrity cell mechanical metamaterial with metal rubber

Qicheng Zhang, Dayi Zhang, Yousef Dobah, Fabrizio Scarpa, Fernando Fraternali, and Robert E. Skelton

Supplementary Information

S1. Model

The tensegrity metamaterial here proposed is different from a classical tensegrity prism:
(1) The top and bottom strings of the tensegrity are constrained by the plates and cannot deform freely, and should therefore be considered rigid compared to the cross strings.
(2) The joints between plates and struts are not ideal pin joints; this introduces added stiffness and friction effects.
(3) The stiffness and damping property of the struts with MR may be different from the ones of the pure MR specimens because of the friction between sleeves and bars.

The base model developed here is based on the force-displacement relations illustrated in [1]. To account for the friction in the bars and the coupled twisting-uniaxial deformations created by the specific joint-plates designs used in the tensegrity metamaterial concept, the original model has been modified as follows:

1. A rotational spring is added to each joint to cater for the additional stiffness introduced on the real joints by the tensegrity design;
2. A friction element that can totally describe the friction introduced by joints, sleeves and test rig compression plate is introduced;
3. The large stiffening of the top and bottom strings induced by the design is represented by an extremely large Young's modulus (10^5 GPa) of those two strings compared to the others (210 GPa).

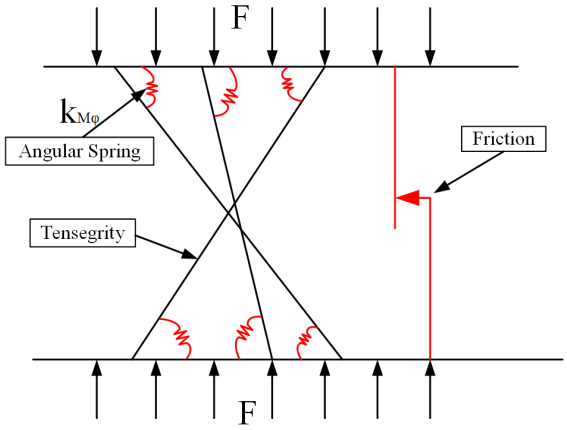

Figure S1. Layout of the modified tensegrity model.

The moment introduced by the angular spring is expressed as following:

$$M_{\varphi} = F_M b = k_{M\varphi}\left(\varphi_h - \varphi_{h0}\right) \quad \text{(S.1)}$$

Where F_M is the equilibrium force generated on the joints by the moment, *b* is the length of the strut, $k_{M\varphi}$ is the rotational stiffness, φ_h is the angle between the strut and plate ($\varphi_h = \arcsin\left(\frac{h}{b}\right)$), *h* is the height of the tensegrity and φ_{h0} is the angle between strut and plate at the undeformed state of the tensegrity. The equilibrium force of moment F_M can be decomposed along the x, y, z Cartesian directions by considering the angles φ_h and θ(torsion angle of the tensegrity).

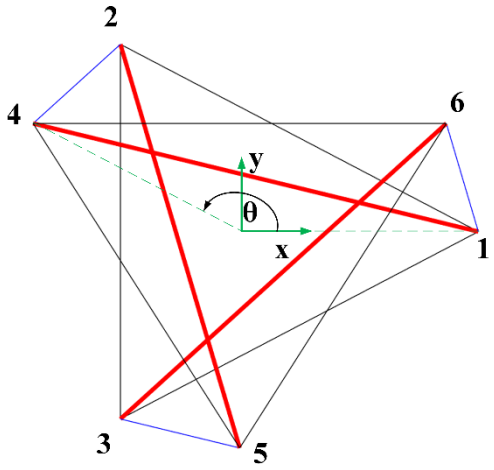

Figure S2. Torsion angle of the tensegrity.

By adding the equilibrium of moments in the Cartesian system and the friction force in the original set of equilibrium equations of [1], one obtains a new set of equilibrium conditions. The friction force (F_f) is different during the loading and unloading phases. In normal classic friction models, the friction force is expressed as the function of the relative displacement between two objects in contact. However, in this model, the friction element represents the combined friction in joints, sleeves and compression plates; this global friction effect cannot be described directly by using normal classic friction models. We impose therefore that the equivalent friction force is expressed into loading (F_{fl}) and unloading terms (F_{fu}) as:

$$F_{fl}(F) = \begin{cases} \alpha F & (F \le F_1) \\ \alpha F_1 + \beta(F - F_1) & (F > F_1) \end{cases}$$
$$F_{fu}(F) = \begin{cases} \beta F & (F \le F_2) \\ \beta F_2 + \alpha(F - F_2) & (F > F_2) \end{cases} \qquad \text{(S.2)}$$

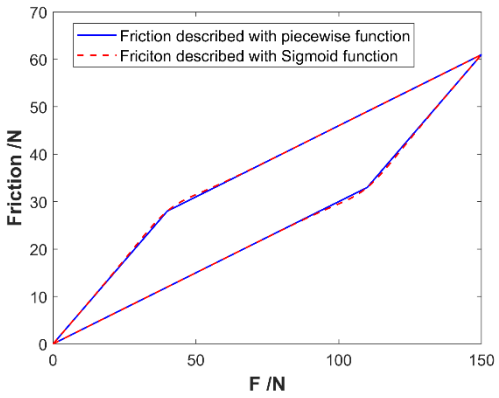

Figure S3. Friction model used in the tensegrity metamaterial

During loading, when $F \le F_1$ the contact friction is considered under stick conditions and the friction force is linearly proportional to the external force *F,* with a stick friction coefficient α . When $F > F_1$, the contact element is in slip condition. In normal contact models, the friction force $F_{fslide} = \mu N$ is constant with the slide (μ is the coefficient of sliding friction and *N* represents the normal contact force). In the friction element of this tensegrity model the normal contact force *N* increases with the external loading force *F*. That means that the sliding friction force should increase with F, even though the contact model enters slip conditions. We therefore assume that the sliding friction force is linearly dependent from the external force *F*, with a sliding friction coefficient β . If F_0 is the maximum loading force, and the end of the hysteretic loop we have $F_{fl}\left(F_0\right) = F_{fu}\left(F_0\right)$, which substituted in (S.2) yeilds $F_0 = F_1 + F_2$. Thus, three unknown parameters α, β and F_1 are sufficient to describe the friction model. To guarantee the derivability and therefore the numerical stability of the solution of the equilibrium equations we use a sigmoid function of the type $S\left(x\right) = \dfrac{1}{1+e^{-ax}}$ to represent the piecewise polynomials in (S.2). The use of the sigmoid into S.2 in the equilibrium equations (S.1) and in [1] leads to a new set of nonlinear equilibrum equations with four unknowns $k_{M\varphi}$, α, β and F_1, which need to be identified from the experimental data. We have used a Particle Swarm method to minimize the objective function $p\left(k_{M\varphi}, \alpha, \beta, F_1\right) = \sum_{n=1}^{7}\left(x\left(F_n\right) - x_n\right)^2 + q\left(\alpha, \beta\right)$, where:

$$q\left(\alpha,\beta\right) = \begin{cases} 0 & \left(\alpha > \beta\right) \\ 10^7 & \left(\alpha \le \beta\right) \end{cases} \qquad \text{(S.3)}$$

The results of the optimization are illustrated in Table S1, with the direct comparison between numerical and experimental hysteretic loops present in Figure 2 of the manuscript.

Table S1. Results from the optimization routine.

Parameters	$k_{M\varphi}$ (N.mm)	α	β	F_1 (N)	Optimized object function value	Loss factor	
						Tested	Calibrated model
Tensegrity without MR	53394	0.7466	0.5	60	0.046	0.127	0.129
Tensegrity with MR	10000	0.7216	0.5	60	0.149	0.164	0.155

S2. Modal analysis and vibration transmissibility

Vibration transmissibility was carried out mounting the tensegrity configurations over an electrodynamic shaker, with the transmissibility measured between the output (top) and input (bottom) accelerometres (PCB). The shaker was excited using a white noise (bandwidth 1-500 Hz, input voltage 0.1 V corresponding to 0.7 g r.m.s.).
Table S1 shows the natural frequencies obtained from the hammer test.

Table S2. Results from the modal analysis of the tensegrity configurations.

Mode	Tensegrity without MR /Hz	Tensegrity with MR /Hz
1	20	20
2	74	73
3	205	200
4	235	218
5	252	228
6	280	266
7	332	320

The first mode for the two configurations is a torsion one; the horizontal transmissibility corresponding to the 20 Hz peak (Figure S3b) has a significantly higher amplitude than the vertical one (Figure S3A). This result is also confirmed by performing trial sine sweep tests (frequency range 1-250 Hz, sweeping rate of 0.2 Hz/s, input voltage 0.1 V). The second mode for the two configurations (74 Hz and 73 Hz) is an dilatational one along the vertical direction.

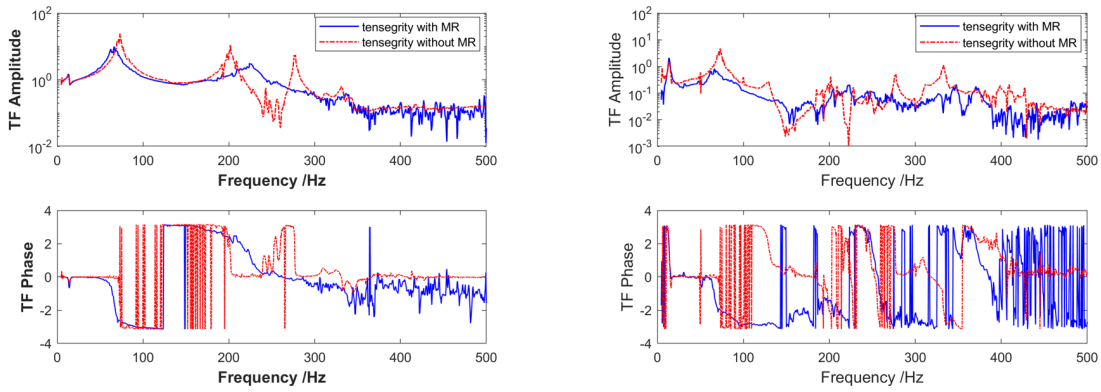

Figure S4. Bode plots for (a) vertical and (b) horizontal transmissibility of the two tensegrity configurations.

String resonances were measured exciting the tensioned wires with an impulse and measuring the natural frequency with a microphone. The resonances were at. A Finite

Element model (Figure S5a) has been developed to better understand the modal contributions from the plates. The model is based on the ANSYS Rel. 16.0 code (elements SHELL181). Boundary conditions consist in rigid simple supports at the three corners. The eigenvalues and eigenmodes have been extracted using a Lanczos method.The first natural frequency is at 270 Hz, and the corresponding mode is an out-of-plane bending one (Figure S5b). This mode may correspond to the 262 Hz – 280 Hz observed in the modal analysis. Higher modes of the plate are at 415 Hz and 427 Hz, all related to torsional and couple twist-bend.

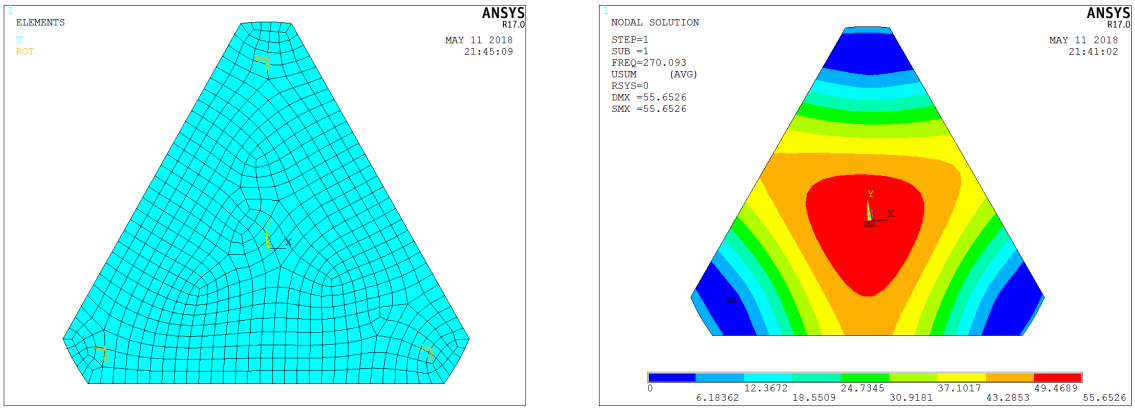

(a) (b)

Figure S5. (a) FEM model of the plate; (b) numerical 1st plate mode (out-of-plane bending) from the FE model

Reference:

1. Fraternali, F., G. Carpentieri, and A. Amendola, *On the mechanical modeling of the extreme softening/stiffening response of axially loaded tensegrity prisms.* Journal of the Mechanics and Physics of Solids, 2015. **74**: p. 136-157.